Contribution of Monthly and Regional Rainfall to the Strength of Indian Summer Monsoon

YANGXING ZHENG AND M. M. ALI

Center for Ocean–Atmospheric Prediction Studies, Florida State University, Tallahassee, Florida

MARK A. BOURASSA

Department of Earth, Ocean, and Atmospheric Science, and Center for Ocean–Atmospheric Prediction Studies, Florida State University, Tallahassee, Florida

(Manuscript received 14 September 2015, in final form 18 March 2016)

ABSTRACT

Indian summer monsoon rainfall (ISMR; June–September) has both temporal and spatial variability causing floods and droughts in different seasons and locations, leading to a strong or weak monsoon. Here, the authors present the contribution of all-India monthly, seasonal, and regional rainfall to the ISMR, with an emphasis on the strong and weak monsoons. Here, regional rainfall is restricted to the seasonal rainfall over four regions defined by the India Meteorological Department (IMD) primarily for the purpose of forecasting regional rainfall: northwest India (NWI), northeast India (NEI), central India (CI), and south peninsula India (SPIN). In this study, two rainfall datasets provided by IMD are used: 1) all-India monthly and seasonal (June–September) rainfall series for the entire Indian subcontinent as well as seasonal rainfall series for the four homogeneous regions for the period 1901–2013 and 2) the latest daily gridded rainfall data for the period 1951–2014, which is used for assessment at the extent to which the four regions are appropriate for the intended purpose. Rainfall during July–August contributes the most to the total seasonal rainfall, regardless of whether it is a strong or weak monsoon. Although NEI has the maximum area-weighted rainfall, its contribution is the least toward determining a strong or weak monsoon. It is the rainfall in the remaining three regions (NWI, CI, and SPIN) that controls whether an ISMR is strong or weak. Compared to monthly rainfall, regional rainfall dominates the strong or weak rainfall periods.

1. Introduction

The Indian economy, to a major extent, depends upon the all-India summer monsoon rainfall. Because of differential heating of the Indian subcontinent and the adjoining water bodies during summer, moisture is drawn from the ocean to produce a monsoon that begins in June and ends by September, with intense rainfall during July and August. The rainfall during these four months is defined as Indian summer monsoon rainfall (ISMR; June–September) by the India Meteorological Department (IMD; Attri and Tyagi 2010). Approximately 75% of the total (12 months) annual all-India rainfall is received during these four months (Oza and Kishtawal 2014). ISMR is a weighted average of the June–September (JJAS) rainfall at well-distributed rain gauge stations across India (Parthasarathy et al. 1992, 1995). Although the interannual variation of ISMR has a standard deviation of only about 10% of the mean, it has a very large impact on agricultural production in India (Gadgil 2003). Even though the all-India monsoon rainfall does not vary hugely from year to year, it has large monthly and regional variations. Dash et al. (2002) report that the spatial variations of rainfall vary from 8.5% in northeastern India to 27% in northwestern India. While some parts of the country get excess rainfall, causing floods during one part of the season, some other sectors face a serious deficiency and experience droughts. Similarly, if one month gets heavy rainfall, another month can experience a break in the monsoon, leading to a small amount of rainfall.

Earlier studies (Sikka and Gadgil 1980; Pant and Parthasarathy 1981; Rasmusson and Carpenter 1983)

Corresponding author address: Yangxing Zheng, Center for Ocean–Atmospheric Prediction Studies, Florida State University, 2000 Levy Ave., Rm. 259, Building A, Tallahassee, FL 32306.
E-mail: yzheng@fsu.edu

DOI: 10.1175/MWR-D-15-0318.1

reported a close correspondence between deficit monsoon rainfall and El Niño. However, Kumar et al. (1999) suggested that the link with El Niño has weakened in the last decade. While some studies (e.g., Zhou and Lau 2001; Krishnamurthy and Shukla 2000; Donohoe et al. 2014) have attempted to understand the interannual and decadal variation of rainfall, no attempt has been made to study which month of the monsoon season and which region of the Indian subcontinent contributes most significantly to the total ISMR. This study addresses these questions. In addition to the direct contribution of monthly and regional rainfall magnitude to the total ISMR during strong or weak monsoons, another important question remains unanswered: is it possible for a strong or weak monsoon to be determined from the monthly and/or regional rainfall? In this study, for the first time, we attempt to answer this question using monthly average and area-weighted regional rainfall data from IMD, with special reference to the strong and weak monsoons. For an improved regional rainfall forecast, the IMD defined four so-called homogeneous regions across India: northwest India (NWI), northeast India (NEI), central India (CI), and south peninsula (SPIN). These four regions were selected based on meteorological records (prepared on the basis of 306 fixed well-distributed rain gauges in the plain regions of India) indicating that the variation in rainfall over each of the meteorological subdivisions that make up the region is positively and significantly correlated with the area-weighted rainfall variation over the region as a whole (Parthasarathy et al. 1995). It is important to note that these four regions are defined primarily for the purpose of forecasting regional rainfall and that the rainfall within these four regions is not strictly homogeneous. Nevertheless, researchers (Pattanaik 2007a,b) and the IMD, an official governmental agency, continue to make weather forecasts and to provide rainfall data for these four regions. As discussed in section 8, the four regions defined by the IMD are also a reasonable choice for our intended purpose. In this paper, we attempt to describe how regional rainfalls over the four regions contribute to the ISMR during both the strong and weak monsoon periods, in comparison to the contribution of monthly rainfall. We select regional rainfall over these four regions for analysis because the rainfall over each region is relevant to regional rainfall forecast across India, and we hope to understand the importance of regional rainfall over these regions in characterizing the strength of ISMRs. It should be noted that the present study is not intended to seek the physical mechanisms responsible for the potential differences between strong and weak ISMRs; hence, we do not attempt to interpret why the contributions of monthly rainfall and/or regional JJAS rainfalls are more important to the total ISMR. Instead, we simply present a descriptive analysis of rainfall data prepared by the IMD to reveal objectively the relative importance of monthly rainfall and regional JJAS rainfall to the strength of ISMRs. Some hypotheses regarding the physical mechanisms are provided in the discussion section and will serve as a basis for our future work.

The remainder of this paper is organized as follows. The datasets and methods used in this study are described in section 2. Section 3 presents the distribution of all-India monthly rainfall and seasonal area-weighted rainfall over the four regions during four extreme strong and weak monsoons, as well as during all strong and weak monsoon years. Changes in monthly rainfall and seasonal mean rainfall over the four regions during the four most extreme strong and four most extreme weak monsoons as compared to those during all strong and weak monsoon periods are also provided in section 4. In section 5, an objective statistical significance testing the differences in monthly rainfall across India and regional JJAS rainfall over each region between strong and weak ISMRs is provided. Salient features of the probability density function (PDF) of monthly ISMR distribution and seasonal mean rainfall in the four regions are discussed in section 6. Roles of monthly rainfall and regional JJAS rainfall in contributing to a strong or weak ISMR are discussed in section 7. Section 8 assesses the extent to which the four regions defined by IMD are appropriate for this study and further provides some hypotheses regarding the physical mechanisms responsible for rainfall distribution over the regions. Finally, a summary is presented in section 9.

2. Data and methods

In this study, two rainfall datasets provided by IMD have been used: 1) all-India monthly and seasonal (June–September) rainfall series and seasonal rainfall series for the four regions over the period 1901–2013 and 2) the latest daily gridded ($1° \times 1°$) rainfall data for the period 1951–2014, which is used to assess the extent to which the four regions are appropriate for this study.

In this study, a strong ISMR year is when the total all-India JJAS rainfall of a calendar year is more than 10% of the all-India mean JJAS rainfall averaged over the years 1901–2013 (i.e., 898 mm). Similarly, a weak ISMR year is when the total all-India JJAS rainfall of a calendar year is less than 10% of the all-India mean JJAS rainfall averaged over the years 1901–2013. A normal ISMR year is when the departure of the total all-India JJAS rainfall for the year from the long-term mean value is within ±10% of the mean value. Figure 1 shows

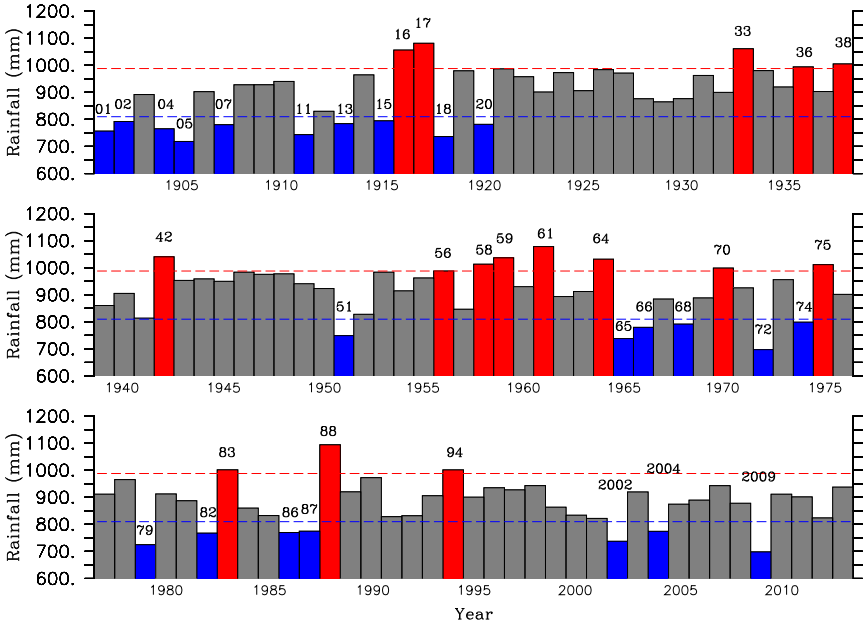

FIG. 1. Evolution of JJAS Indian rainfall (mm) over the period 1901–2013. Strong (red bars), weak (blue bars), and normal (gray bars) ISMRs are identified by the departure of JJAS rainfall of each year from the JJAS rainfall climatology computed over the period 1901–2013, whose departure values are larger than +10%, smaller than −10%, and within ±10% of the seasonal climatology, respectively. The red (blue) dashed line denotes a value of 110% (90%) of seasonal climatology (i.e., 898 mm), which is 988 mm (808 mm). The years of strong and weak ISMRs are denoted by the numbers over the bars.

the evolution of all-India seasonal (JJAS) rainfall for the period 1901–2013 with strong, weak, and normal ISMR years identified according to the above definitions. The rainfall in strong, weak, and normal monsoons is denoted by red, blue, and gray bars, respectively. During 1901–2013, there are 16 strong ISMR years, 23 weak ISMR years, and 74 normal ISMR years. The years of strong and weak ISMRs are denoted at the top of the bars in the figure. Clearly, normal rainfall occurs during approximately 65% of the years (i.e., 74 out of 113

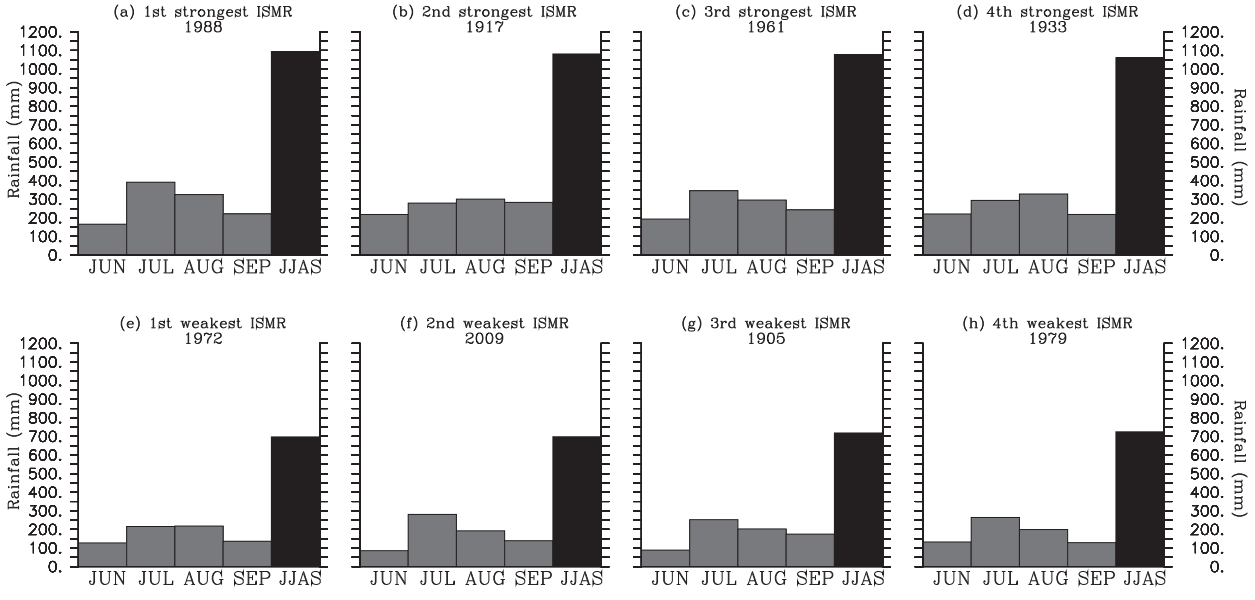

FIG. 2. Monthly rainfall distribution during (a)–(d) the four strongest ISMR years and (e)–(h) the four weakest ISMR years.

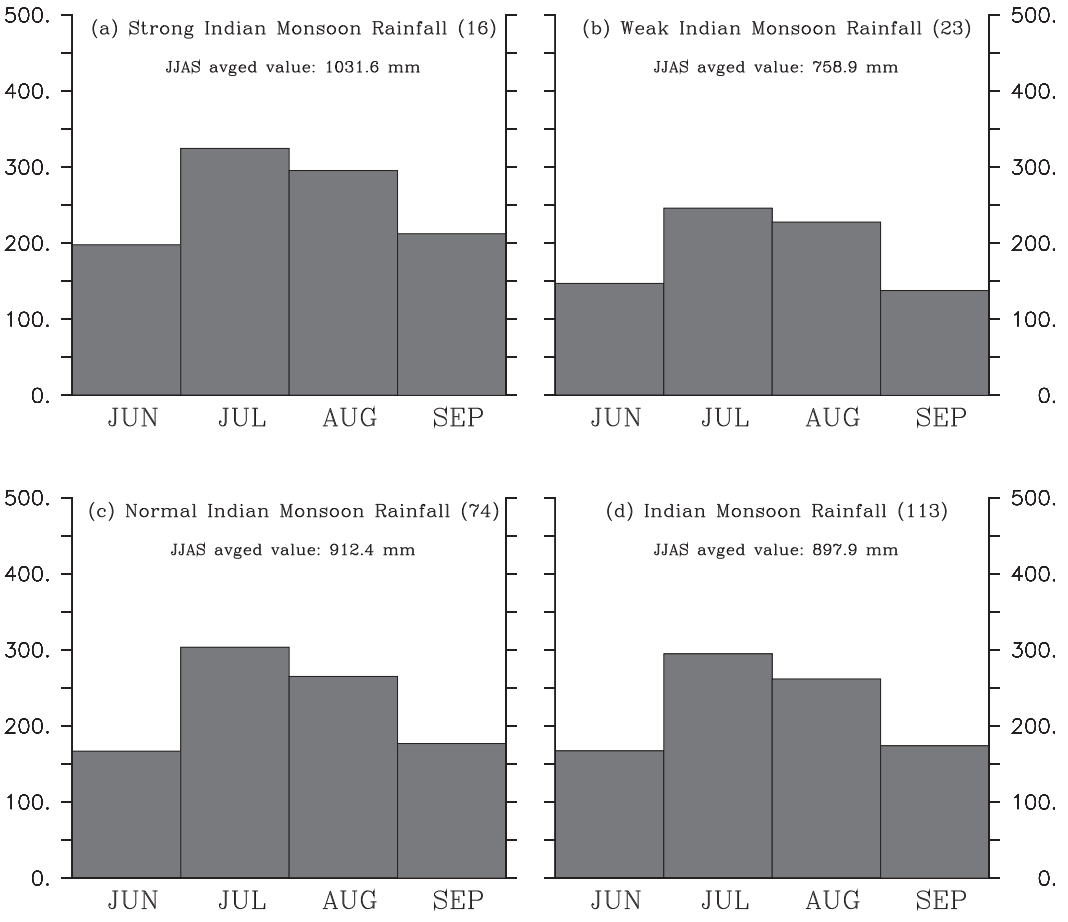

FIG. 3. Composites of monthly rainfall distribution based on (a) 16 strong ISMRs, (b) 23 weak ISMRs, (c) 74 normal ISMRs, and (d) all 113 years.

years), although India has experienced frequent floods and droughts in different regions and different seasons. This implies that considering regional distribution of seasonal rainfall is more important than considering the seasonal rainfall over the entire country of India as one unit. Hence, in the following sections we describe the salient features of monthly and regional rainfall with special reference to strong and weak monsoons. The Wilcoxon–Mann–Whitney rank sum test, a nonparametric test, is applied to examine whether the monthly and regional rainfall differences between strong and weak monsoons are statistically significant. Based on these features, we discuss the contribution of monthly and regional rainfall to the strength of Indian summer monsoon rainfall.

3. Monthly and regional JJAS rainfall distribution

a. Monthly rainfall distribution

To understand the contribution of each month during the extreme monsoons, we first examine the monthly rainfall distribution in the four strongest (1988, 1917, 1961, and 1933) and the four weakest (1972, 2009, 1905, and 1979) monsoon years (Fig. 2). During the heaviest rainfall years, either July or August contributes the maximum to the total ISMR, followed by September and June, except in 1933, wherein rainfall in June is more than that in September. This scenario also exists during the weakest rainfall years, except in 1979, wherein rainfall in June is slightly more than that in September. However, the rainfall in each month during the strongest ISMR years is always larger than that during the weakest ISMR years. The above features are also seen when they are averaged over 16 strong and 23 weak ISMR years (Fig. 3). Similar to the individual strong and weak ISMR years, averaged monthly rainfall during strong monsoons is larger than that during weak monsoons. Monthly rainfall averaged over normal ISMR years is very close (within ±3%) to the long-term mean values primarily because the normal ISMR years dominate the whole analysis period.

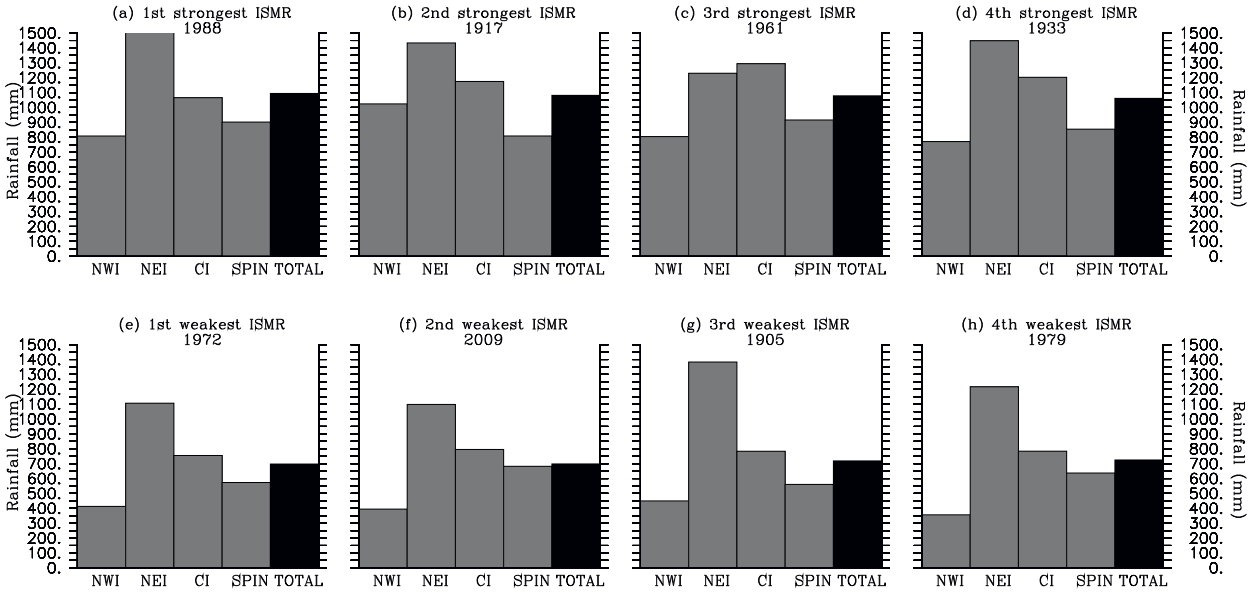

FIG. 4. Seasonal rainfall distribution in the four homogeneous regions for (a)–(d) the four strongest ISMR years and (e)–(h) the four weakest ISMR years.

b. Regional JJAS rainfall distribution

In addition to understanding the monthly distribution during strong and weak ISMR years, it is worth studying how the rainfall is apportioned in different regions during strong and weak monsoons. Figure 4 displays seasonal (i.e., JJAS) rainfall distribution in these four regions during the same extremely strong and weak monsoon years as shown in Fig. 2. During the strongest ISMR years, area-weighted rainfall in NEI is generally the greatest, followed by rainfall in CI, SPIN, and NWI, except in 1961, in which rainfall in CI is slightly larger than that in NEI, and in 1917, in which rainfall in NWI is larger than that in SPIN. Such common features also exist during the weakest ISMR years. Dash et al. (2002) observed that spatial variation is least (8.5%) within NEI and highest within NWI (22.7%). Thus, rainfall in NEI that has the greatest impact on ISMR has the least spatial variability and rainfall in NWI with the least impact on ISMR has the greatest spatial variability. To see the common features of JJAS rainfall in these four regions, the JJAS rainfall in these regions is averaged over 16 strong, 23 weak, and 74 normal ISMR years, as compared to the long-term mean of JJAS rainfall (Fig. 5). Results indicate that the largest area-weighted JJAS rainfall occurs in NEI, followed by CI, SPIN, and NWI, regardless of whether it is during strong, weak, or normal ISMR years. In addition, the actual rainfall during strong ISMR years in these four regions is always larger than that in the same region during weak ISMR years. For example, during strong ISMR years, the averages of JJAS rainfall in NEI, CI, SPIN, and NWI are 1388, 1148, 832, and 764 mm, respectively, compared to 1303, 807, 626, and 472 mm, respectively, during the weak ISMR years. Clearly, with the exception of NEI, changes in rainfall between strong and weak ISMR years are small compared to the other three regions, which will be further discussed in section 4.

4. Changes in monthly all-India rainfall and regional JJAS rainfall

In the previous section we examined the monthly and regional distribution of actual rainfall for strong and weak ISMR years. To understand in which month(s) and in which region(s) the rainfall can greatly influence the strength of the total ISMR, in this section we investigate and compare the changes of rainfall in each month of the monsoon season and over these four regions between strong and weak ISMR years. In this section we show that the changes in monthly all-India rainfall and regional rainfall can determine a strong, weak, or normal ISMR for a given year if such changes are significant.

a. Changes in monthly all-India rainfall

Changes in monthly all-India rainfall are represented by the ratios (in percent) of monthly rainfall to the corresponding monthly climatology. The changes of monthly rainfall during the four strongest and the four weakest ISMR years are displayed in Fig. 6. The monthly climatology is computed over the period 1901–2013. With the exception of July 1917, there is an overall increase in

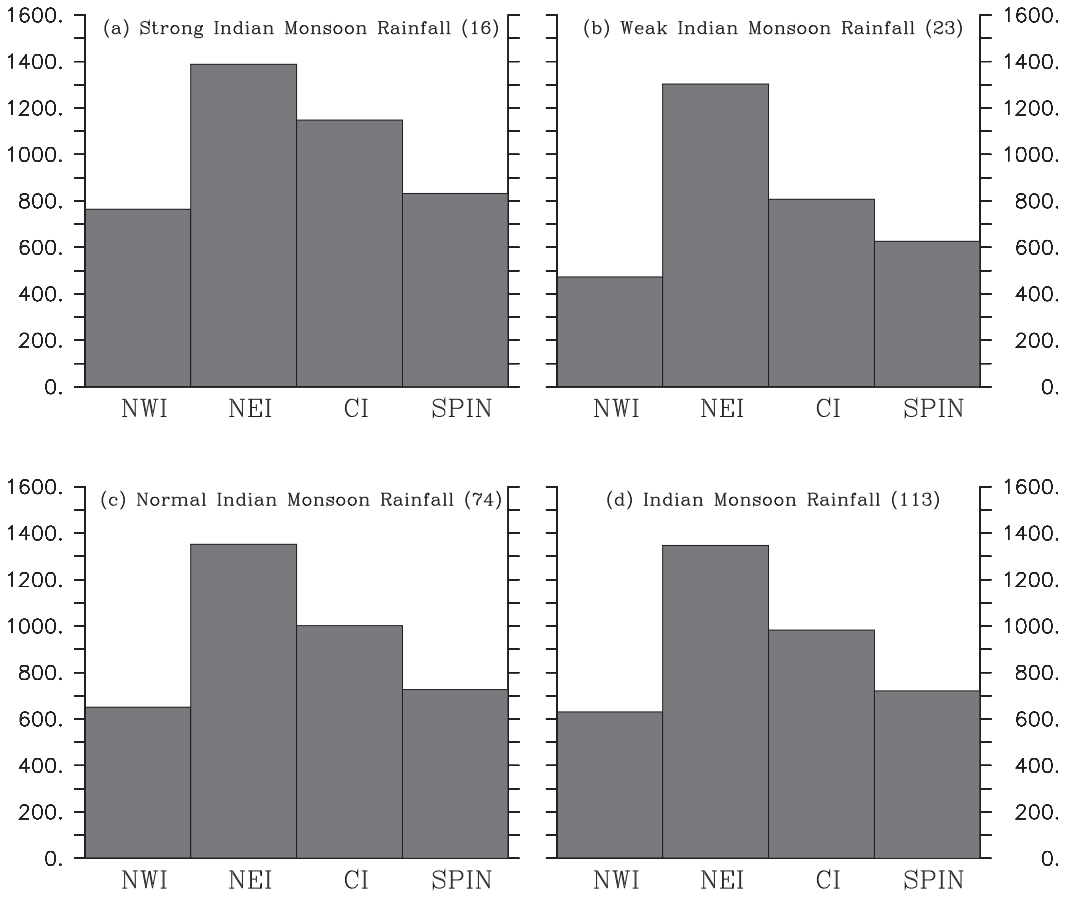

FIG. 5. Composites of seasonal rainfall distribution in the four homogeneous regions based on (a) 16 strong ISMRs, (b) 23 weak ISMRs, (c) 74 normal ISMRs, and (d) all 113 years.

rainfall in June–September during the strongest ISMR years, and there is an overall decrease in rainfall in June–September during the weakest ISMR years relative to the corresponding climatology. For these eight extreme ISMR years, the largest increase or decrease relative to the corresponding climatology in rainfall magnitude can happen during the onset phase (June), the mature phase (July–August), and the withdrawal phase (September). Changes in averaged monthly rainfall (Fig. 7) over 16 strong, 23 weak, and 74 normal ISMR years also show similar features, with an overall increase rainfall in June–September during strong ISMR years and an overall decrease rainfall in June–September during weak ISMR years, as seen in Fig. 6. Although absolute magnitude of actual rainfall during the mature phase (i.e., July–August) makes the greatest contribution to the total ISMR (Figs. 2, 3), rainfall has the greatest increase relative to the corresponding monthly climatology during the onset and withdrawal phases (i.e., June and September, respectively) in strong ISMR years, while rainfall during the withdrawal phase represents the largest overall reduction relative to the corresponding monthly climatology in weak ISMR years. It should be pointed out that rainfall in normal ISMR years is very close to the corresponding climatology. In addition to the relative changes, the monthly rainfall departures from the corresponding monthly climatology for 16 strong, 23 weak, and 74 normal ISMR years are illustrated in Fig. 8. It is clear that the actual rainfall increases from about 28 to 40 mm during 16 strong ISMR years, in which September has the largest increase (~37 mm). Interestingly, the actual rainfall decrease has a wider range (20–50 mm), in which July has the largest reduction (~48 mm), followed by September (~36 mm). In summary, during strong ISMR years, although rainfall in each month increases as a whole with a similar magnitude, there are relatively larger changes during the onset and withdrawal phases with reference to its corresponding monthly climatology. During weak ISMR years, while July has the largest reduction in actual rainfall, September has the largest reduction relative to its climatological value.

b. *Changes in regional JJAS rainfall*

Changes of JJAS rainfall over the four regions (NWI, NEI, CI, and SPIN) relative to the JJAS climatology in

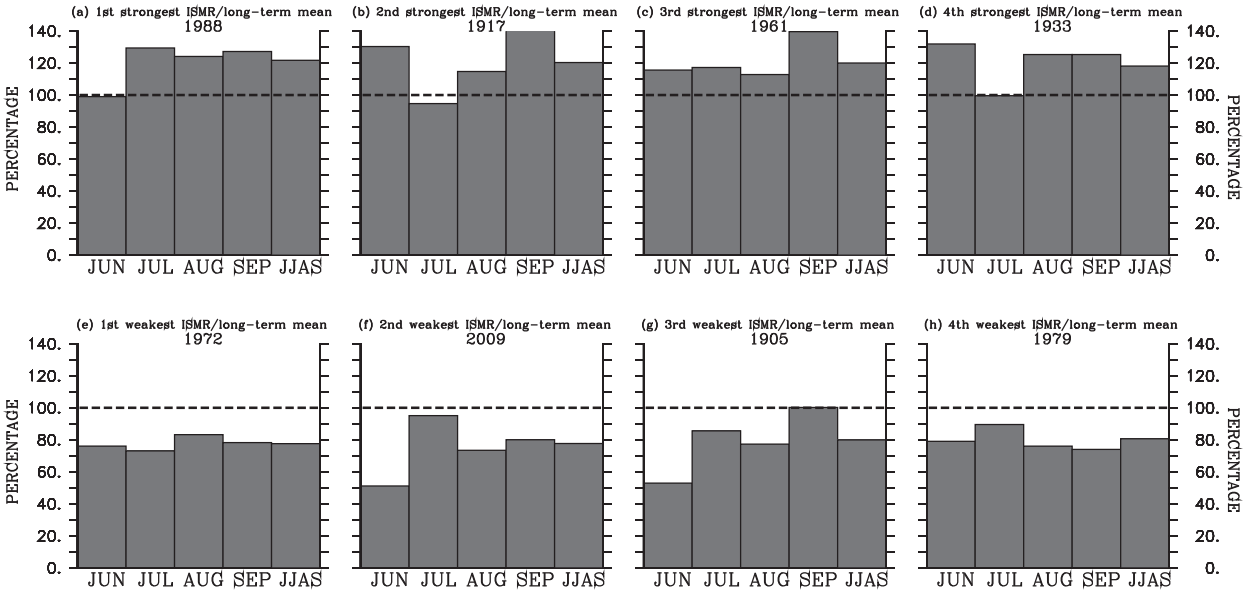

FIG. 6. Ratios (%) of monthly rainfall distribution during (a)–(d) the four strongest ISMR years and (e)–(h) the four weakest ISMR years to the corresponding monthly climatology computed based on the period 1901–2013. The black dashed line denotes the value of 100%.

the corresponding region for the four strongest and four weakest ISMR years are displayed in Fig. 9. With reference to the seasonal climatology, rainfall in the NWI, NEI, CI, and SPIN regions is uniformly more during the four strongest ISMR years, except in 1961, in which rainfall is slightly less in the NEI region, although 1961 is one of the strongest ISMR years. Meanwhile, rainfall in these four regions is uniformly less during the four weakest ISMR years, except in 1905, in which rainfall is slightly more in the NEI region, although this year is one of the weakest ISMR years. The lack of sensitivity of JJAS rainfall over NEI to the strength of ISMRs implies that using JJAS rainfall in NEI cannot clearly indicate the strength of the ISMRs. JJAS rainfall over NWI has the largest change relative to its seasonal climatology for the above eight years, implying that the changes of JJAS rainfall in NWI may serve as a tool to identify a strong or weak ISMR. Average rainfall (Fig. 10) over 16 strong, 23 weak, and 74 normal ISMR years also illustrates similar features with an overall increase in seasonal rainfall during strong monsoon years and an overall decrease in seasonal rainfall during weak monsoon years, as seen in Fig. 9. The JJAS rainfall in these four regions averaged over normal ISMR years is almost equal to that averaged over the entire period (Fig. 10c) because the normal ISMR years dominate over the entire period. The largest change in rainfall for both strong and weak monsoon years is seen in NWI, although the actual area-weighted rainfall is the least over NWI. By contrast, the smallest change in rainfall during both strong and weak monsoons is seen in NEI, although the actual area-weighted rainfall is the largest over NEI. These striking features are seen in Fig. 5. JJAS rainfall departures from the corresponding JJAS climatology in these four regions for both strong and weak monsoon years (Fig. 11) indicate that the change of actual area-weighted rainfall in CI is the largest, followed by NWI, and the change of actual area-weighted rainfall in NEI is the least for both strong and weak ISMRs. During normal ISMR years, JJAS rainfall changes in the four regions relative to the long-term mean values are very small, with the largest changes of about 20 mm in NWI (Fig. 11c).

It is interesting to examine the overall changes of regional JJAS rainfall in these four regions and the changes of monthly rainfall for 16 strong, 23 weak, and 74 normal ISMR years, which are represented by the ratios (in percent) to the all-India JJAS rainfall climatology. Table 1 summarizes the results. The drops in rainfall from strong to weak ISMR years in NWI, NEI, CI, and SPIN are 32.43%, 9.5%, 38.02%, and 22.94%, respectively. Clearly, rainfall in the NEI region has the smallest change between strong and weak ISMR years, implying that this region cannot be used to identify whether an ISMR is strong or weak. The drops in June, July, August, and September rainfall from strong to weak monsoon are 5.66%, 8.74%, 7.64%, and 8.32%, respectively. Change in rainfall during June is the least, indicating rainfall in June has the least contribution to the total ISMR.

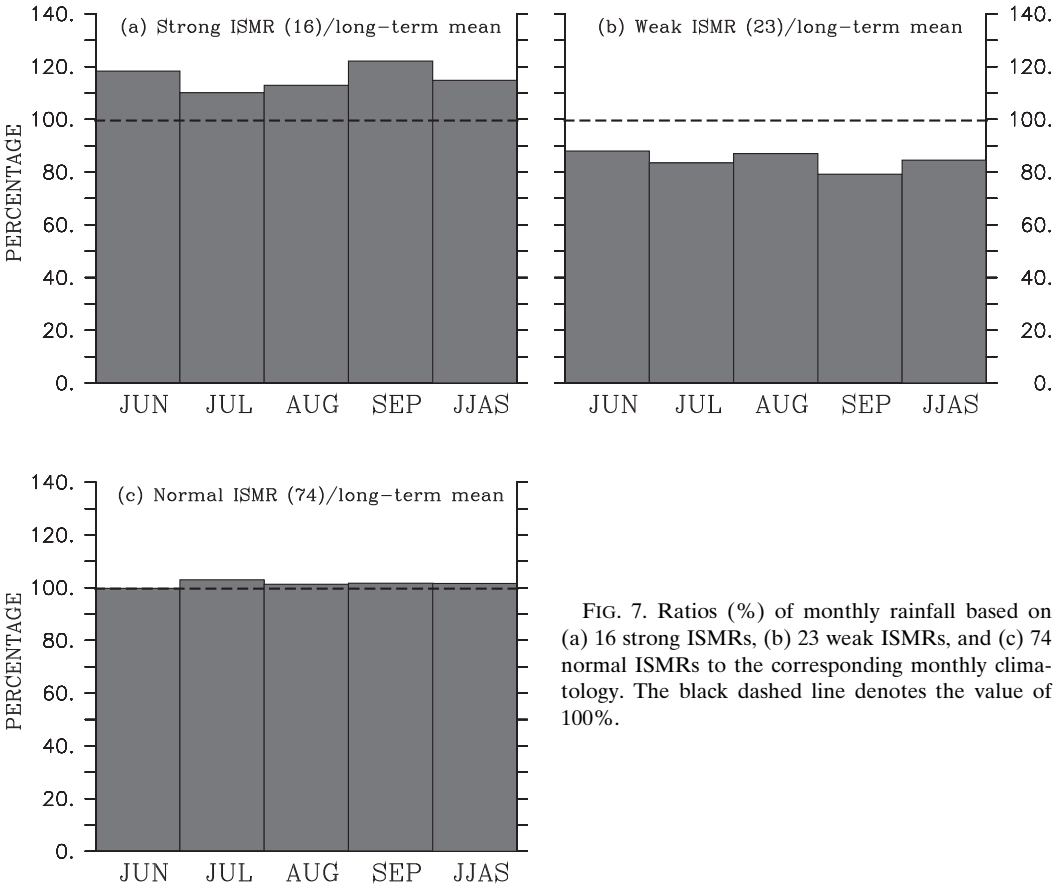

FIG. 7. Ratios (%) of monthly rainfall based on (a) 16 strong ISMRs, (b) 23 weak ISMRs, and (c) 74 normal ISMRs to the corresponding monthly climatology. The black dashed line denotes the value of 100%.

c. *Association of monthly rainfall and regional JJAS rainfall with ISMRs*

Since the strength of ISMRs can be tracked either by the changes of monthly rainfall or by the changes of regional JJAS rainfall as examined above, we further identify the relationship between monthly and regional JJAS rainfall and the strength of ISMRs. Figure 12 is the scatterplot of monthly and regional JJAS rainfall versus the ISMRs over the period 1901–2013. The linear correlation coefficient for each case is denoted in the upper right of each panel. We also compute the slope of a linear best-fitting equation for each case. The slope represents the overall response of monthly and regional JJAS rainfall strength to the variation of ISMRs. In addition, uncertainty of slope is assessed: the smaller the uncertainty, the more confidence in such a linear relationship. Table 2 lists the slope and its uncertainty as well as the linear correlation coefficients. It is evident that rainfall over NWI and CI has the best positive linear correlation (i.e., 0.83) with the strength of ISMR and rainfall over NEI has the poorest correlation (i.e., 0.30). The correlation coefficients of monthly rainfall in July–September are as large as those of rainfall over SPIN. The results indicate that the strength of ISMRs can be better characterized by the strength of regional JJAS rainfall than by monthly rainfall. The uncertainty of slope for regional JJAS rainfall over NWI and CI is the smallest compared to monthly rainfall, which gives us more confidence that the strength of ISMRs is better characterized by the variation of regional JJAS rainfall over NWI and CI, in comparison to monthly rainfall.

5. Statistical significance test on monthly all-India rainfall and regional JJAS rainfall between strong and weak monsoons

An important question arises: are the previously described differences in features of monthly and regional rainfall between strong and weak monsoons statistically significant? Here we utilize the Wilcoxon–Mann–Whitney rank sum test (Corder and Foreman 2014), a nonparametric statistical test, to compare two independent unpaired groups: one for rainfall during strong monsoons and one for rainfall during weak monsoons periods. Such a method is useful when the distributions of samples are not assumed. The null hypothesis is that the rainfall distributions during strong and weak

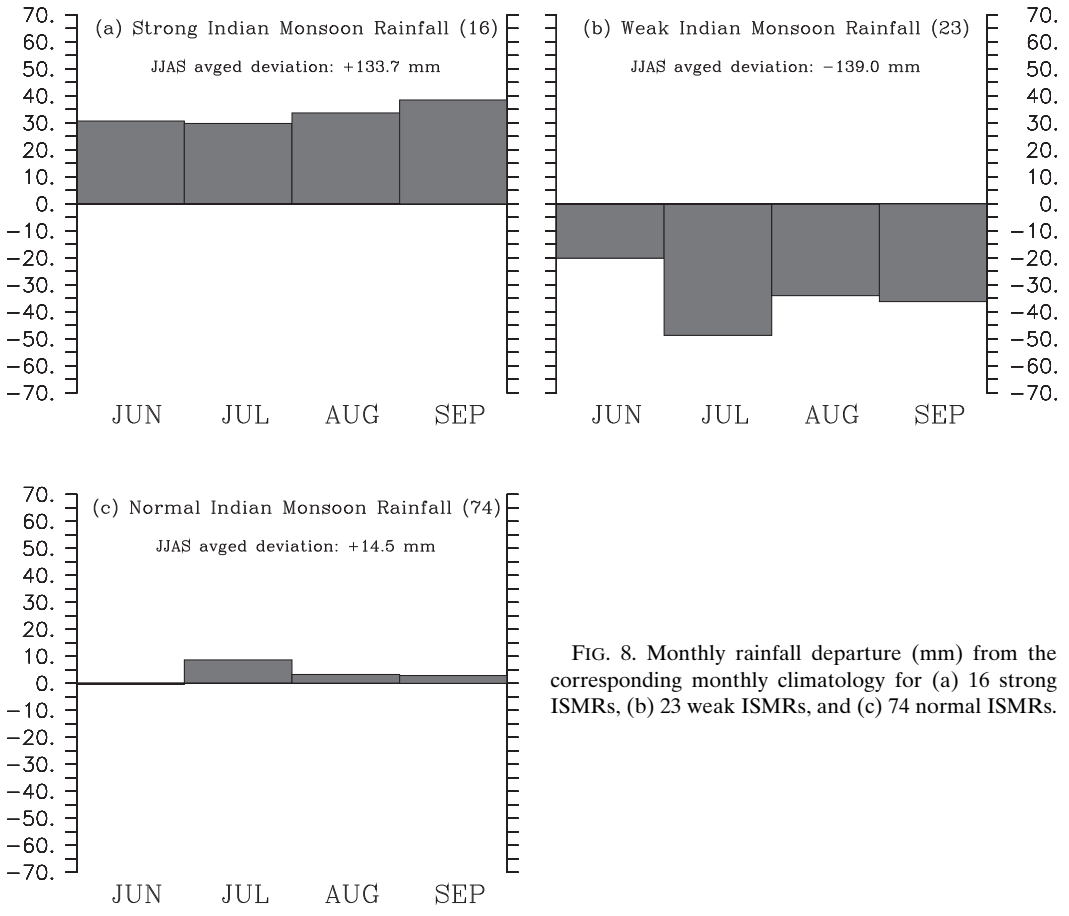

FIG. 8. Monthly rainfall departure (mm) from the corresponding monthly climatology for (a) 16 strong ISMRs, (b) 23 weak ISMRs, and (c) 74 normal ISMRs.

monsoons are identical, so there is a 50% probability that an observation from a value randomly selected from one population exceeds an observation randomly selected from the other population. In this study, we present a one-sided alternative hypothesis that the distributions of monthly rainfalls and regional JJAS rainfalls that occurred during strong monsoons are stochastically and significantly greater than the distributions of those that occurred during weak monsoons at a given confidence level.

To perform the test, we rank all the rainfall values for each case from low to high during 16 strong ($n_1 = 16$) and 23 ($n_2 = 23$) weak monsoon years, regardless of to which group each value belongs. The smallest rainfall value gets a rank of 1, and the largest number gets a rank of n, where $n = n_1 + n_2 = 39$, the total number of rainfall values in the two groups if no tie exists. We then compute the sums of ranks of rainfall for strong and weak monsoons, which are R_1, R_2, respectively. If the mean of R_1 is much larger than the mean of R_2, then the p value will be smaller. The Mann–Whitney U values are computed for strong and weak monsoon years, which are U_1 and U_2, respectively: $U_1 = R_1 - n_1(n_1 + 1)/2$, or $U_2 = R_2 - n_2(n_2 + 1)/2$. The U statistic is approximately Gaussian since $n_1 > 10$ and $n_2 > 10$. To test that the null hypothesis is verified and the mean μ and standard deviation σ of the U statistic are determined,

$$\mu = n_1 n_2/2 \quad \text{and} \quad \sigma = [n_1 n_2(n_1 + n_2 + 1)/12]^{0.5}.$$

Hence, we obtain a Z score: $Z = (U_1 - \mu)/\sigma \sim N(0, 1)$. We apply a 99% confidence level for a Gaussian distribution to accept or reject the null hypothesis. Table 3 summarizes the results addressing whether the rainfall values during strong ISMRs are significantly larger than those during weak ISMRs. Table 3 clearly shows that monthly all-India rainfalls from June through September during 16 strong ISMRs are significantly greater than those of the corresponding month during 23 weak ISMRs. Interestingly, with the exception of those over NEI, the regional JJAS rainfalls over NWI, CI, and SPIN during 16 strong ISMRs are also significantly larger than those over the corresponding region during 23 weak ISMRs at a 99% confidence level.

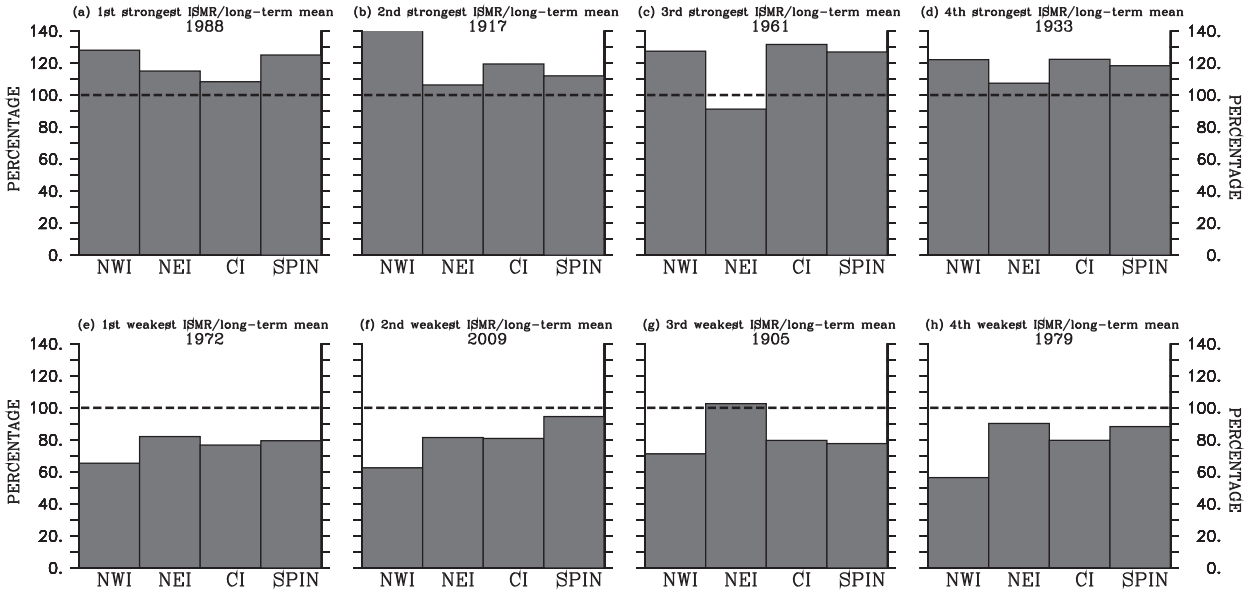

FIG. 9. Ratios (%) of seasonal rainfall in the four homogeneous regions during (a)–(d) the four strongest ISMR years and (e)–(h) the four weakest ISMR years to the seasonal climatology in the corresponding regions. The black dashed line denotes the value of 100%.

6. PDF distribution of all-India monthly and regional JJAS rainfall

To understand what causes the changes in all-India monthly rainfall and JJAS rainfall in the four regions between strong and weak monsoons (as discussed in the previous sections), we calculate the probability density function of all-India monthly rainfall and of seasonal rainfall in these regions. We first examine the PDF distribution of monthly rainfall from June through September based on 16 strong, 23 weak, and 74 normal ISMR years and all 113 years of datasets (Fig. 13). The PDF distribution of monthly rainfall in strong ISMR years is, to some degree, different from that in weak ISMR years, as can be clearly seen in the JJAS rainfall PDF distribution. The PDF distribution in normal ISMR years is similar to that of all ISMR years. The PDF distribution differs during each phase between strong and weak ISMR years. Specifically, in the mature phase (July–August) of strong ISMR years, large monthly rainfall (250–400 mm) is most frequent, and in the mature phase of weak ISMR years, relatively small monthly rainfall (200–300 mm) is most frequent. Monthly rainfall (150–250 mm) is dominant during the onset and withdrawal phases of the strong ISMR years, and the dominant monthly rainfall range is 100–200 mm during the onset and withdrawal phases of weak ISMR years. The discrepancies in PDF distribution of monthly rainfall between strong and weak monsoons help interpret the differences of all-India rainfall change in the different months of summer season between strong and weak monsoons as shown in Table 1.

The large difference in PDF distribution of JJAS rainfall in the four regions between strong and weak ISMR years, if exists, may help identify the role of rainfall in each of the four regions in the strength of the total ISMR. Here we present the PDF distribution of JJAS rainfall in the four regions based on 16 strong, 23 weak, and 74 normal ISMR years, as well as the entire 113 years of rainfall datasets (Fig. 14). Clearly, the PDF distribution of seasonal rainfall in NWI, CI, and SPIN is significantly different between strong and weak ISMR years, while there is not such a large difference in NEI. General speaking, the relatively large JJAS rainfall in NWI, CI, and SPIN occurs more frequently during strong ISMR years than during weak ISMR years. Specifically, a large rainfall range of 1000–1400 mm is most frequent in CI during the strong ISMR years, while this range reduces to 700–1000 mm during the weak ISMR years. In NWI, a rainfall range of 600–800 mm is most frequent in the strong ISMR years, and in the weak ISMR years a rainfall range of 300–600 mm is more typical. In SPIN, a rainfall range of 700–1000 mm occurs most frequently during the strong ISMR years, while in the weak ISMR years, the rainfall falls mostly within the 400–800-mm range. In NEI, large amounts of rainfall (>1400 mm) occur more frequently during the strong monsoon years as compared to the weak monsoon years. Such a distinctive PDF distribution in different regions between strong and weak ISMR years clearly indicates the importance of spatial distribution of rainfall in the

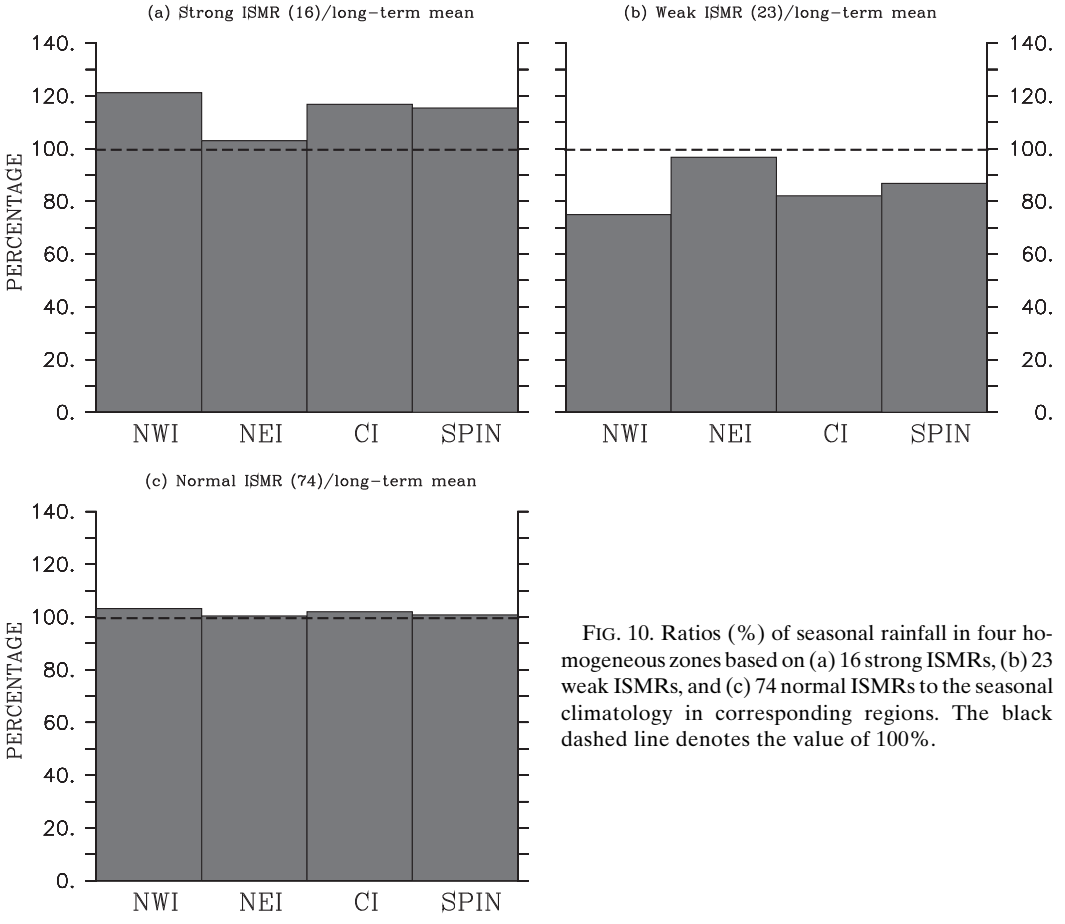

FIG. 10. Ratios (%) of seasonal rainfall in four homogeneous zones based on (a) 16 strong ISMRs, (b) 23 weak ISMRs, and (c) 74 normal ISMRs to the seasonal climatology in corresponding regions. The black dashed line denotes the value of 100%.

production of a strong or weak ISMR. In summary, it is the frequency of large, medium, and small rainfall in CI, NWI, and NWI that determines whether an ISMR is strong or weak. Compared to the other three regions, the PDF distribution in CI is most distinct and the PDF distribution in NEI is least distinct between strong and weak ISMR years. Thus, CI is the most dominant region in determining whether an ISMR is strong or weak. Both the narrow rain range in NEI (Figs. 10, 11, Table 1) and the resemblance of rainfall occurrence frequency in NEI between strong and weak ISMR years (Fig. 14) indicates that rainfall in NEI cannot be used to determine whether an ISMR is strong or weak.

7. Yearly variation of all-India monthly and regional JJAS rainfall

In this section, we examine the interannual variability of all-India monthly rainfall and regional JJAS rainfall in the four regions. For this purpose, we computed the ratio of all-India rainfall in June–September to the long-term mean JJAS rainfall (Fig. 15) and the ratio of JJAS rainfall in the four regions to the long-term mean JJAS rainfall in the corresponding regions (Fig. 16). This analysis further confirms our conclusion, detailed in the preceding section, that spatial/regional distribution of rainfall is more important than the temporal distribution in determining whether an ISMR is strong or weak.

It is clear that the percentages in July–August (i.e., mature phase) are larger than those in June (i.e., onset phase) and September (i.e., withdrawal phase; Fig. 15). This is expected because rainfall during a mature phase always provides the largest contribution to the total ISMR, as seen in Figs. 2 and 3. The amplitude of yearly variation of monthly rainfall is represented by one standard deviation of monthly rainfall time series over the period 1901–2013. Surprisingly, the yearly variations of rainfall during the onset, mature, and withdrawal phases (i.e., June, July–August, and September, respectively) are very similar, with one standard deviation of approximately 4%. In other words, resemblance of yearly variation of monthly rainfall does not provide a clear indication of whether an ISMR is strong or weak.

In contrast, there are distinct features tied to yearly variation of JJAS rainfall in the spatial distribution (Fig. 16). These results show that yearly variation of

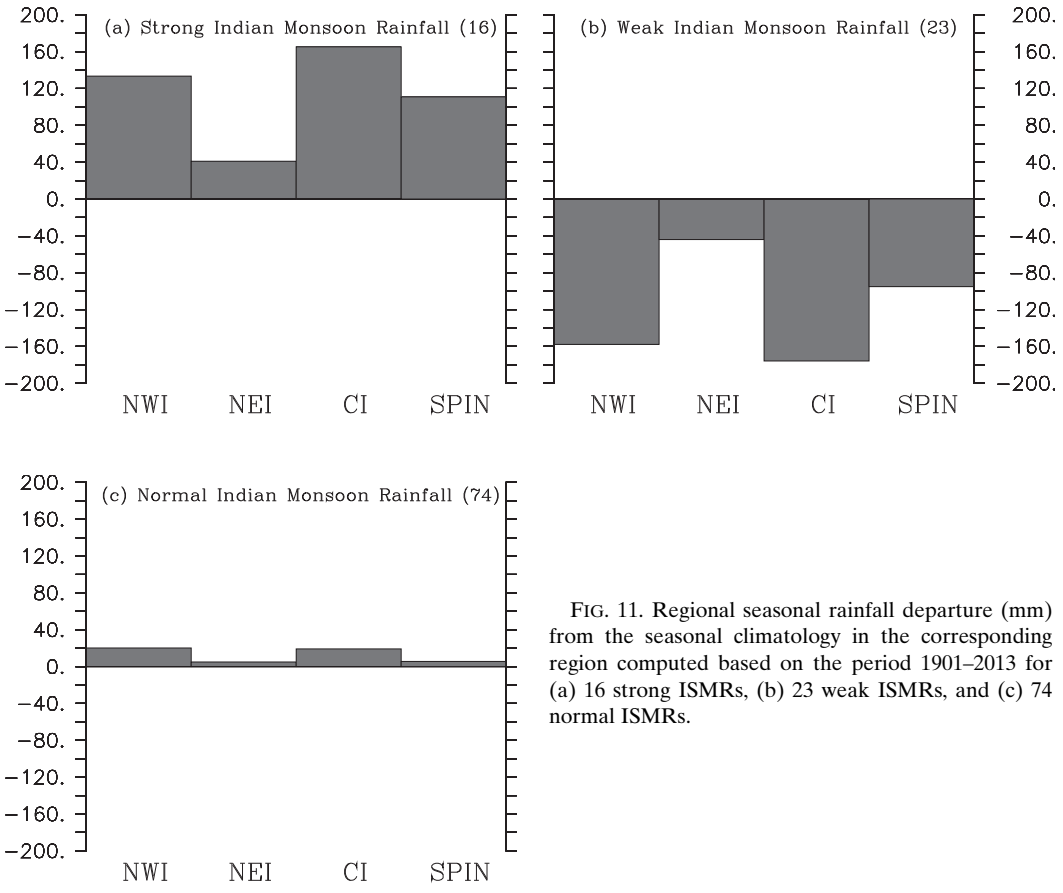

FIG. 11. Regional seasonal rainfall departure (mm) from the seasonal climatology in the corresponding region computed based on the period 1901–2013 for (a) 16 strong ISMRs, (b) 23 weak ISMRs, and (c) 74 normal ISMRs.

seasonal rainfall in NEI is much smaller than that in NWI (which is the largest), CI, and SPIN. Consequently, seasonal rainfall in NEI provides the least contribution to the yearly variation of total ISMR, and the interannual variability of total ISMR is primarily caused by the variations of JJAS rainfall in NWI, CI, and SPIN. Interestingly, the relative strength of yearly variations for monthly rainfall and for regional JJAS rainfall is consistent with the change of monthly rainfall and regional JJAS rainfall between strong and weak ISMR years (Table 1). Therefore, compared to the rainfall distribution in June, July, August, and September, JJAS rainfall distribution in NWI, CI, and SPIN appears to play an important role in determining whether there is a strong or weak ISMR.

8. Discussion

The above conclusions would hold if the selected regions were perfect homogeneous regions. However, it is difficult to define an ideal homogeneous rainfall region in the Indian subcontinent since there is no unambiguous definition regarding the ''homogeneity.'' The homogeneity of rainfall in space can be defined based on the mean and variability at different time scales. In this study, we used rainfall series over the four so-called homogeneous regions defined by IMD, and we discussed the contribution of regional seasonally mean rainfall time series as well as all-India monthly rainfall to the strength of Indian summer monsoons. Such a selection is

TABLE 1. Ratios (in %) of all-India monthly rainfall and seasonal rainfall over the four homogeneous regions to the seasonal climatology of all-India rainfall (i.e., 898 mm) computed over the period 1901–2013 for 16 strong, 23 weak, and 74 normal ISMRs.

	Strong ISMRs (16)	Weak ISMRs (23)	Normal ISMRs (74)
Regions			
NWI	85.09%	52.66%	72.48%
NEI	154.6%	145.1%	150.6%
CI	127.9%	89.88%	111.6%
SPIN	92.66%	69.72%	80.93%
Months			
Jun	22.05%	16.39%	18.59%
Jul	36.15%	27.41%	33.80%
Aug	32.91%	25.37%	29.52%
Sep	23.67%	15.35%	19.70%
JJAS	114.8%	84.52%	101.6%

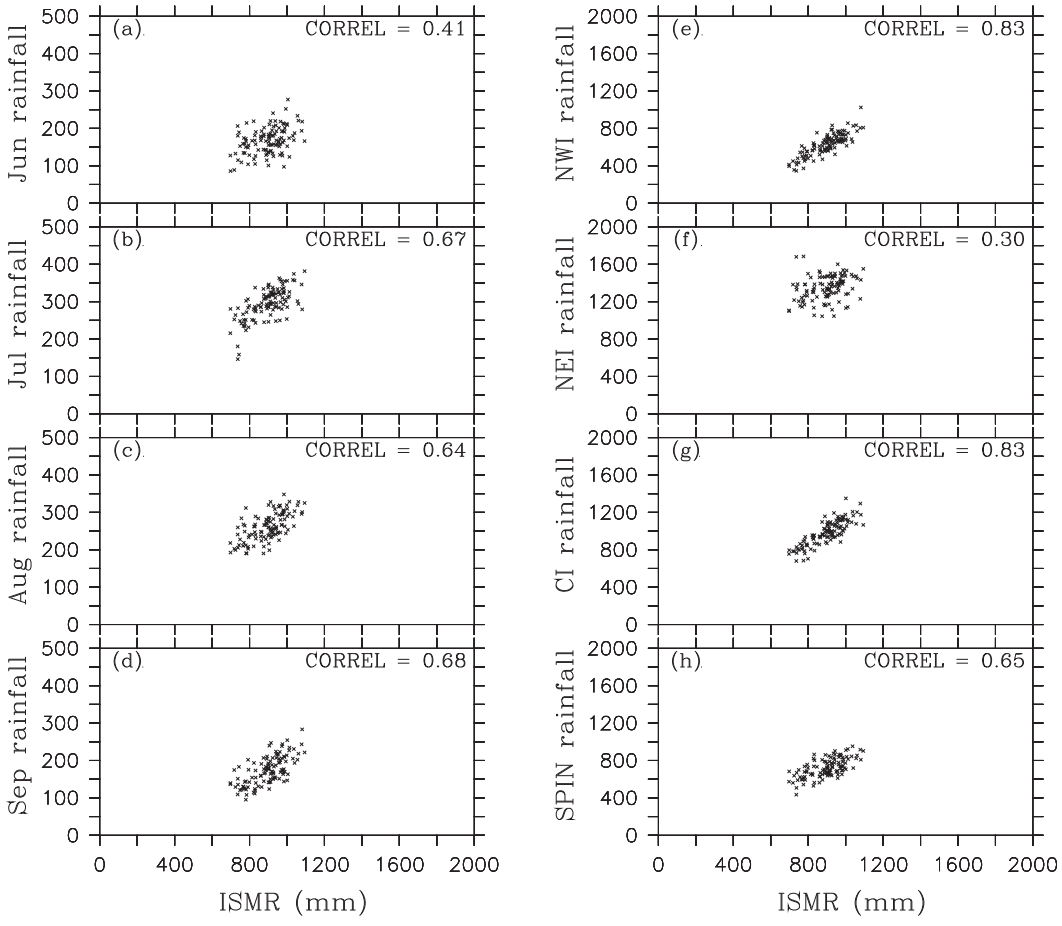

FIG. 12. Scatterplot of (a)–(d) monthly rainfall and (e)–(h) regional JJAS rainfall vs ISMRs for the period 1901–2013. The linear correlation coefficient is denoted in the upper right of each panel.

appropriate for this particular study if the seasonal mean rainfalls within each of the four selected regions have distinct features between strong and weak monsoons, show some coherence in space, and are distinguishable from other adjacent regions. To assess the extent to which the four regions defined by IMD are appropriate for this study, we computed the seasonally mean rainfall differences between strong and weak Indian summer monsoons using the latest daily gridded rainfall provided by IMD available for the period 1951–2014 (Fig. 17). A statistical significance test (i.e., Student's *t* test) was performed to examine whether the seasonal mean rainfall difference within the selected region between strong and weak monsoons shows some degree of coherence in space and is distinguishable from other adjacent regions (Fig. 17c). Figure 17a illustrates the map of so-called homogeneous rainfall zone of India defined by IMD projected onto 1° × 1° grids of daily rainfall dataset. Figure 17b shows the spatial distribution of ratio (in percentage) of seasonally mean rainfall differences to the all-India mean rainfall (i.e., 898 mm). Figure 17b illustrates that the Indian subcontinent can be roughly classified into the four so-called ''homogeneous'' regions defined by IMD in terms of seasonally mean rainfall differences between strong and weak

TABLE 2. Uncertainty in slope for all-India monthly rainfall and seasonal rainfall over the four homogeneous regions vs ISMRs during 1901–2013.

	Slope (uncertainty)	Correlation coefficient
Regions		
NWI	1.084 (±0.052 61)	0.83
NEI	0.432 (±0.090 59)	0.30
CI	1.195 (±0.052 52)	0.83
SPIN	0.714 (±0.072 16)	0.65
Months		
Jun	0.159 (±0.086 72)	0.41
Jul	0.302 (±0.070 68)	0.67
Aug	0.261 (±0.072 71)	0.64
Sep	0.278 (±0.069 95)	0.68

TABLE 3. The Wilcoxon–Mann–Whitney rank sum test regarding whether monthly all-India rainfall and regional JJAS rainfall over the four homogeneous regions during 16 strong ISMRs are significantly greater than those during 23 weak ISMRs at a 99% confidence level.

	Critical Z value	Significant (yes or no)
Regions		
NWI	5.254	Yes
NEI	2.027	No
CI	5.254	Yes
SPIN	5.254	Yes
Months		
Jun	3.541	Yes
Jul	4.569	Yes
Aug	4.512	Yes
Sep	4.826	Yes

monsoons. The rainfall within each selected region shows some degree of coherence in space and is distinguishable from other adjacent regions in some sense. For example, CI represents a region where most of the seasonal mean rainfall differences are larger than 40%. NWI also has a peak ratio (greater than 40%) north of 30°N. NWI and CI are bounded by the ratio of 20%–40% in the region 25°–30°N. SPIN shows large ratios along the west coast of the Indian subcontinent (Western Ghats), a salient feature compared to the adjacent region (i.e., CI) and the east coast (Eastern Ghats) of SPIN. Evidently, the rainfall changes over SPIN between strong and weak monsoons in this study are caused by the significant rainfall changes over the Western Ghats between strong and weak monsoons, which is presumably associated with the relatively larger transport of moisture from the Arabian Sea during strong monsoons in comparison to that during weak monsoons. Seasonal mean rainfall differences between strong and weak monsoons over the entire NEI region have very weak ratios (within ±20%; also refer to Table 1) and show both signs, demonstrating that NEI is a completely different region when compared to other three regions. Figure 17c further indicates that the

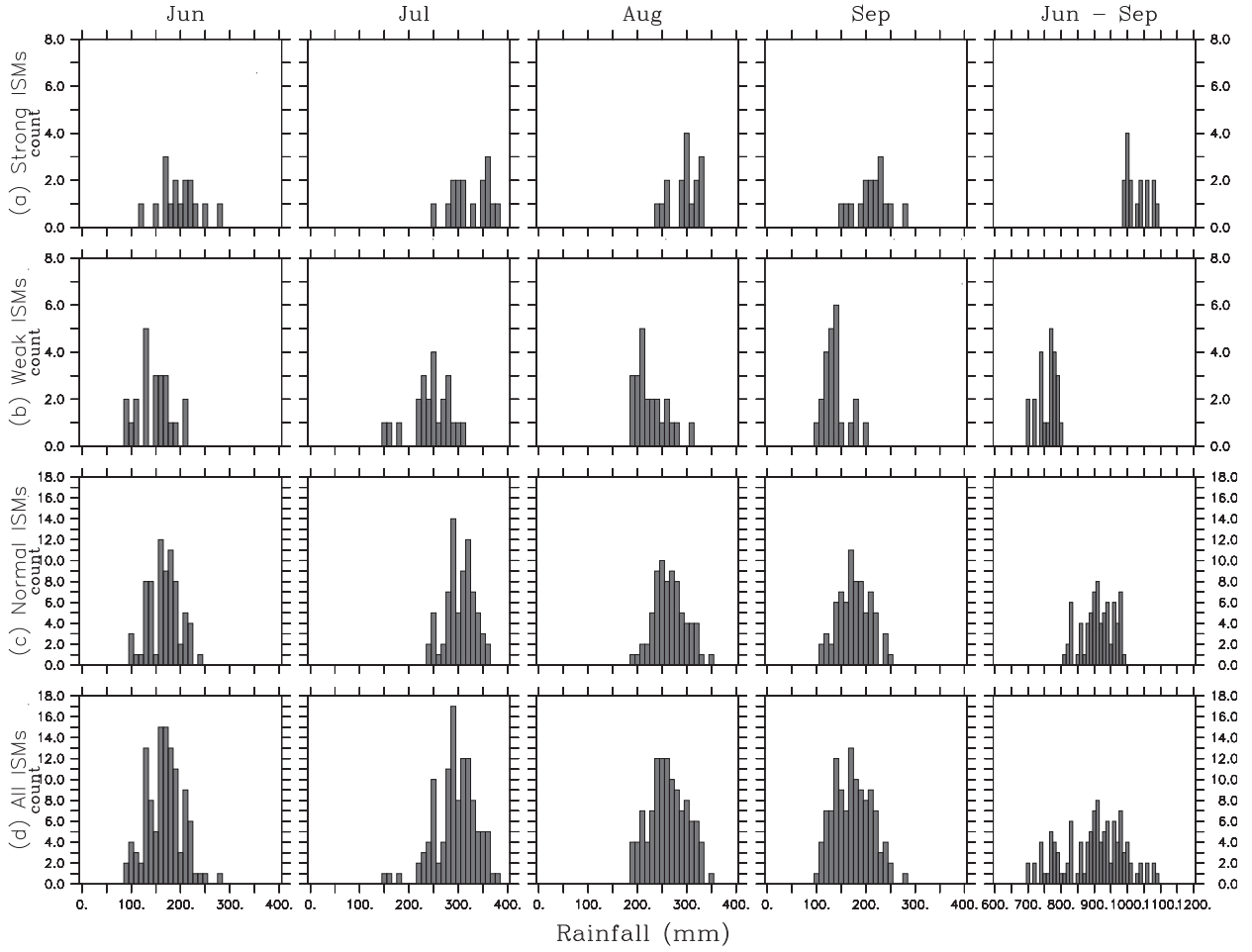

FIG. 13. PDF distribution of monthly rainfall for (a) 16 strong ISMRs, (b) 23 weak ISMRs, (c) 74 normal ISMRs, and (d) all 113 years.

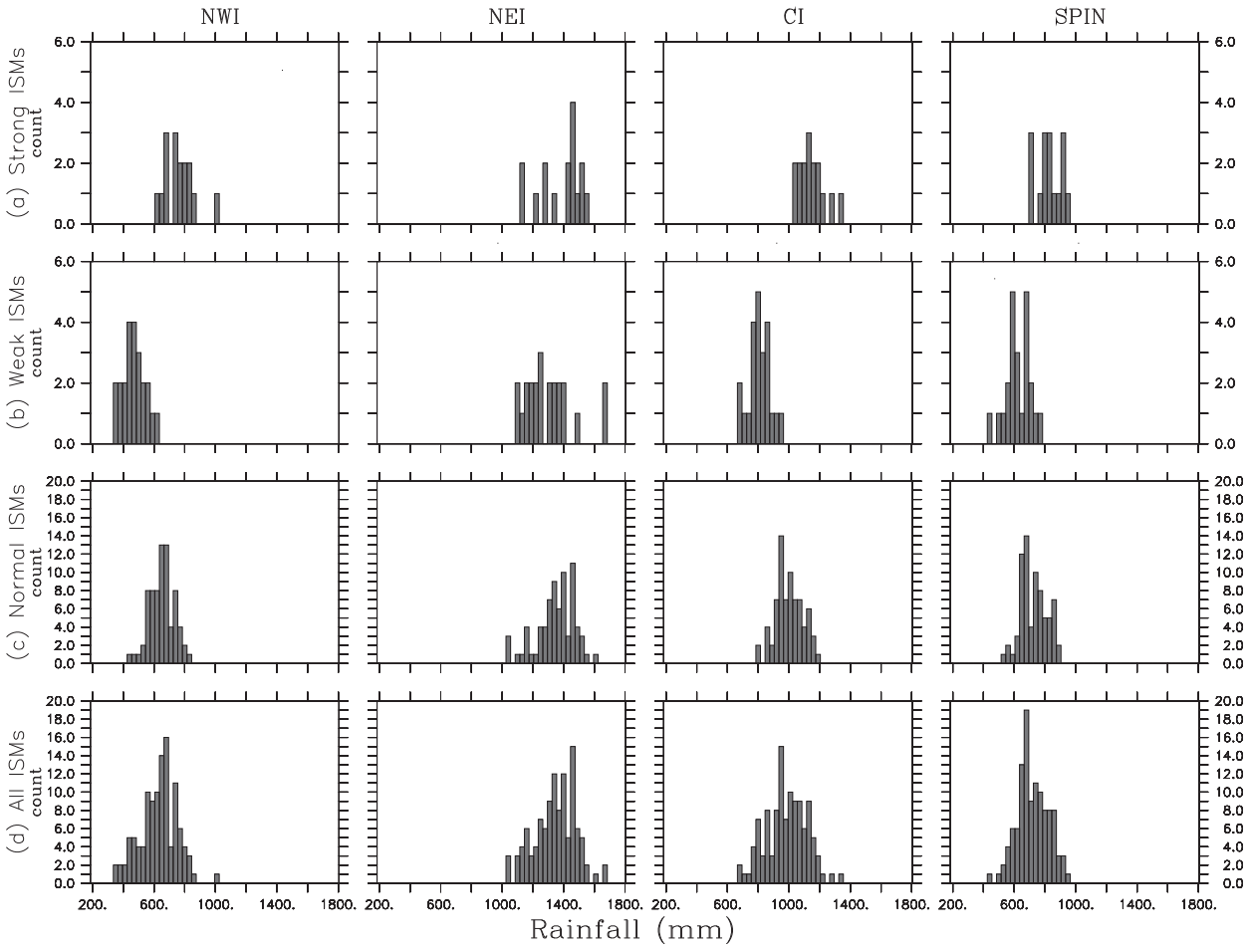

FIG. 14. PDF distribution of regional seasonal rainfall for (a) 16 strong ISMRs, (b) 23 weak ISMRs, (c) 74 normal ISMRs, and (d) all 113 years.

seasonal mean rainfalls during strong monsoons are significantly larger than those during weak monsoons over most of NWI and CI at a 99% confidence level. The seasonal mean rainfall differences between strong and weak monsoons over the Western Ghats of SPIN are dominant and statistically significant at a 99% confidence level, indicating that the seasonal mean rainfall difference over SPIN is primarily caused by the rainfall differences over the Western Ghats. In other words, although rainfall is inhomogeneous within SPIN, the insignificant changes in seasonal mean rainfall between strong and weak monsoons are unimportant to the rainfall changes over the whole SPIN between strong and weak monsoons. Certainly, in terms of rainfall homogeneity, SPIN can be roughly split into two areas: Western Ghats and the rest of SPIN. However, such a partition is not necessary for this particular study. Therefore, the rainfalls over the Western Ghats and Eastern Ghats and the interior of SPIN can be considered as one unit for this particular study. It should be noted that the rainfalls over NWI, CI, and SPIN are well distinguishable from those over NEI because rainfall over NEI shows no significant changes between strong and weak monsoons. This is also true for area-averaged rainfalls over the selected regions (see Table 3). In summary, while IMD defined the four so-called homogeneous rainfall zones primarily for regional rainfall forecasts, the above results demonstrate that such a definition is also appropriate for the purpose of the present study in classifying the Indian subcontinent into four distinct regions in terms of the contribution of seasonally mean regional rainfall to the total strength of ISMRs, even though SPIN includes several distinct regions.

Some hypotheses regarding underlying physical mechanisms controlling the rainfall over the four regions are provided here. For example, physical mechanisms for rainfall over NEI may be similar to those for rainfall over Bangladesh since NEI is adjacent to Bangladesh.

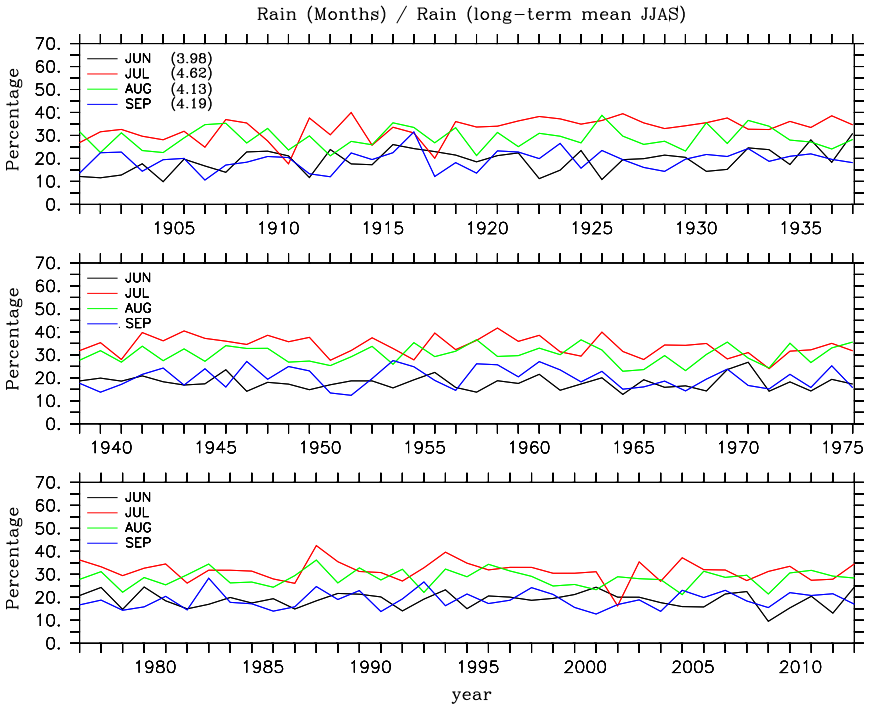

FIG. 15. Evolution of ratios (%) of all-India monthly rainfall to all-India rainfall seasonal climatology. The values in the parentheses in the top panel denote the one standard deviation of the entire time series.

Previous studies (e.g., Gadgil et al. 2011) showed that the average summer monsoon rainfall over Bangladesh is not associated with either the El Niño–Southern Oscillation (ENSO) or the equatorial Indian Ocean oscillation (EQUINOO), while ENSO and EQUINOO are known to play a role in determining the strength of ISMR (Gadgil et al. 2004; Ihara et al. 2007). The remarkable rainfall changes over the Western Ghats of SPIN are closely associated with the orographic impacts as well as the more abundant moisture transported from the Arabian Sea during strong monsoons (versus during weak monsoons), while the weak rainfall changes in other portions of SPIN may be associated with the Bay of Bengal. As revealed in the present study, the rainfall changes over NWI and CI are sufficient to determine the total strength of ISMRs, probably because the physical processes controlling the rainfall over the two regions are closely tied to dominant monsoon processes such as the strength of southwest low-level winds and the supply of moisture primarily from the Arabian Sea. For example, during strong summer monsoons, more moisture is transported from the Arabian Sea by the stronger prevailing southwest winds, which provides more energy to develop and maintain a series of northwestward movement convection systems over the Indian subcontinent that are initiated in the Bay of Bengal. These convection processes play an important role in rainfall strength over CI and NWI since the prevailing track of northwestward convection systems is over CI and NWI. The peak rainfall differences are located north of around 30°N over NWI, while the largest rainfall differences are in the region of 17°–25°N. Although CI and NWI share some common physical processes for rainfall, they have their own locations of peak rainfall changes. It is necessary to unravel these physical mechanisms for the distinction of rainfall changes between strong and weak Indian summer monsoons, which will be the focus of a future study.

9. Summary and conclusions

In this study, the contribution of monthly all-India summer rainfall and seasonal rainfall in the four so-called homogeneous regions (NWI, NEI, CI, and SPIN) to the strength of ISMR is examined using all-India monthly and seasonal mean rainfall as well as seasonal rainfall datasets for the four regions prepared by IMD over the period 1901–2013.

The monthly all-India rainfall series shows that the mature phase (i.e., July–August) contributes the maximum to the total ISMR, whether it is during a strong or weak ISM. Rainfall during the onset phase (i.e., June)

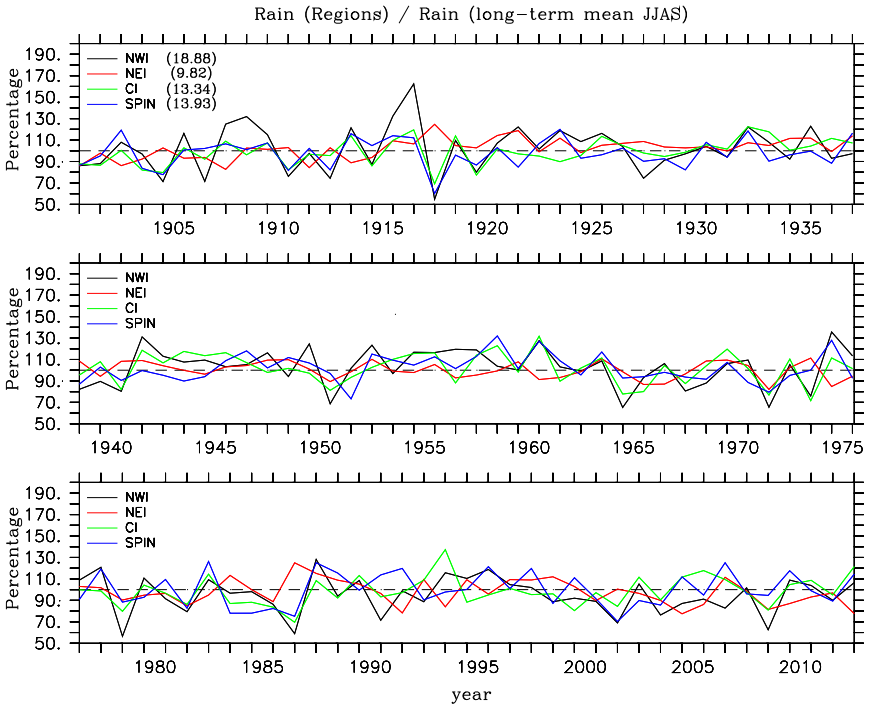

FIG. 16. Evolution of ratios (%) of seasonal rainfall in the four homogeneous regions to its seasonal climatology. The values in the parentheses in the top panel denote the one standard deviation of the entire time series for the four regions.

and withdrawal phase (i.e., September) contributes the least. During strong ISMR years, the rainfall in June–September is generally larger than that in the same months of weak ISMR years (Figs. 2, 3), which is significant at a 99% confidence level (Table 3). The seasonal rainfall series over the four regions confirms that NEI and CI provide the first- and second-largest area-weighted rainfall, respectively, for both strong and weak ISM years. Rainfall in SPIN is slightly greater than that in NWI during both strong and weak ISM years. The seasonal rainfall over the four regions during strong ISMR years is greater than that in the corresponding regions during weak ISMR years (Figs. 4, 5). Except over NEI, the seasonal rainfall over NWI, CI, and SPIN during strong ISMR years is significantly larger than that in the corresponding regions during weak ISMR years at a 99% confidence level (Table 3).

Composite analysis for strong and weak ISMRs indicates that the monthly rainfall in each month is larger than the corresponding monthly climatology (up to a 20% change) during strong ISMR years and smaller than the corresponding monthly climatology during weak ISMR years (also up to a 20% change; Fig. 7). This is also true for most of the months during the individual extreme strongest and weakest ISMR years (Fig. 6). The largest change in monthly rainfall relative to its monthly climatology in any individual ISMR year can happen during the onset phase, the mature phase, and the withdrawal phase for the eight extreme years (Fig. 6). Composite analysis also shows the change of actual rainfall between months during strong ISMR years has a small range (about 30–40 mm), though the change of rain during weak ISMR years has a relatively wider range (about 20–50 mm).Thus, monthly rainfall is not a good indicator of whether an ISMR is strong or weak. In contrast, there are salient features about changes in seasonal rainfall in the four chosen regions between strong and weak monsoons. Composite analysis for JJAS rainfall during strong and weak monsoon years indicates that the seasonal rainfall in each region is larger than the long-term mean seasonal rainfall in the corresponding region during strong monsoons and smaller than the long-term mean seasonal rainfall in the corresponding region during weak monsoons (Fig. 10). This is also true for most selected regions during the individual extreme heaviest and weakest ISMR years (Fig. 9). More importantly, there are distinct changes in seasonal rainfall among these four regions between strong and weak ISMR years. For example, since the actual rain over NEI has the least change in percentage (Fig. 11) relative to the long-term mean of seasonal rainfall (Fig. 10), rainfall variation in NEI does not

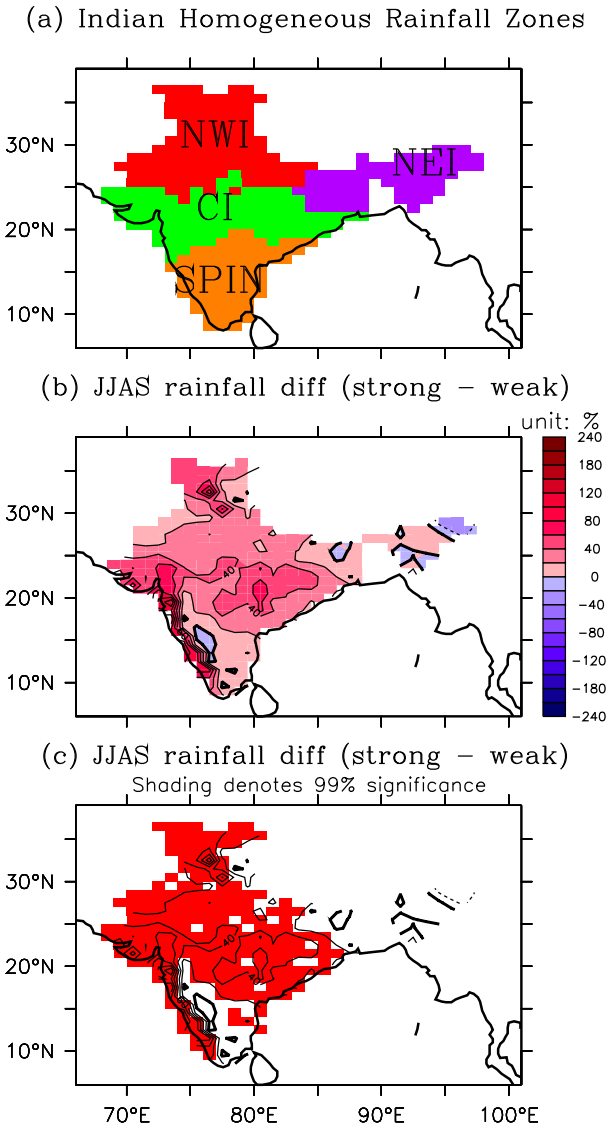

FIG. 17. (a) Homogeneous rainfall regions of India defined by IMD: NWI (red), CI (green), SPIN (orange), and NEI (purple). (b) Spatial distribution of ratio (%) of seasonally mean rainfall differences between strong and weak Indian summer monsoons to the temporal mean of total ISMRs (i.e., 898 mm) over Indian subcontinent. (c) As in (b), but significant portions are shaded in red. The latest daily gridded rainfall data provided by IMD are used for analysis, which is now available for the period 1951–2014.

determine a strong or weak monsoon. Because actual seasonal rainfall over NWI and CI significantly increases during strong monsoons and significantly decreases during weak monsoons compared to the long-term mean (Figs. 10, 11), the significant rainfall changes over NWI and/or CI relative to its seasonal climatology are able to signal whether an ISMR is strong or weak. Compared to monthly rainfall, regional rainfall over NWI and CI has the best linear correlation with ISMRs, along with the smallest uncertainty of such linear relationship over the entire analysis period (Fig. 12, Table 2), which further proves that the strength of ISMR can be better characterized by regional JJAS rainfall rather than by monthly rainfall.

PDF distribution of monthly rainfall is different between strong and weak monsoons (Fig. 13). During the mature phase, a relatively large monthly rainfall (>300 mm) occurs more frequently in strong ISMR years than in weak ISMR years while medium rainfall (200–300 mm) occurs more frequently in weak ISMR years than that in strong ISMR years. During the withdrawal phase, larger monthly rainfall (>200 mm) is more frequent during strong ISMR years, whereas a rainfall range of 100–150 mm is more frequent during weak ISMR years. This leads to a significant difference in September's actual rainfall between strong and weak ISMR years, as seen in Fig. 8. During the onset phase, the PDFs of both strong and weak monsoons are similar, with a common rainfall range of 150–200 mm. On the other hand, the discrepancies in PDF distribution of regional seasonal rainfall between strong and weak monsoons are intriguing (Fig. 14). Rainfall over NEI has a similar PDF distribution between strong and weak monsoons, thus explaining why there is a small change in NEI as seen in Figs. 10 and 11. There are salient differences in PDF distribution of seasonal rainfall over the CI, NWI, and SPIN regions. This explains why rainfall in these three regions significantly increases during strong monsoons and significantly decreases during weak monsoons. Monthly rainfall in June–September has a similar interannual variability (Fig. 15). In contrast, there is large interannual variability of rainfall over the CI, NWI, and SPIN regions (Fig. 16), which indicates that the large fluctuation of rainfall over these three regions can cause a strong or weak ISMR. Therefore, the significant fluctuation of regional rainfall, as compared to the small and similar fluctuation of monthly rainfall, determines whether an ISMR is strong or weak.

Acknowledgments. The authors thank the India Meteorological Department for providing the all-India monthly rainfall and seasonal rainfall in the four homogeneous rainfall zones. Computational facilities were provided by the Center for Ocean–Atmospheric Prediction Studies (COAPS) at Florida State University. The research was supported by the National Aeronautics and Space Administration (NASA) Physical Oceanography support of the Ocean Vector Winds Science Team (OVWST), NASA NEWS, and NOAA/Climate Observing Division (COD).

REFERENCES

Attri, S. D., and A. Tyagi, 2010: Climate profile of India. Met Monograph Environment Meteorology 01/2010, India Meteorological Department, 122 pp.

Corder, G. W., and D. I. Foreman, 2014: *Nonparametric Statistics: A Step-by Step Approach.* 2nd ed. Wiley, 288 pp.

Dash, S. K., M. S. Shekhar, G. P. Singh, and A. D. Vernekar, 2002: Relationship between surface fields over Indian Ocean and monsoon rainfall over homogeneous zones of India. *Mausam*, **53** (2), 133–144.

Donohoe, A., J. Marshall, D. Ferreira, K. Armour, and D. McGee, 2014: The interannual variability of tropical precipitation and interhemispheric energy transport. *J. Climate*, **27**, 3377–3392, doi:10.1175/JCLI-D-13-00499.1.

Gadgil, S., 2003: The Indian monsoon and its variability. *Annu. Rev. Earth Planet. Sci.*, **31**, 429–467, doi:10.1146/annurev.earth.31.100901.141251.

——, P. N. Vinaychandran, P. A. Francis, and S. Gadgil, 2004: Extremes of Indian summer monsoon rainfall, ENSO, equatorial Indian Ocean oscillation. *Geophys. Res. Lett.*, **31**, L12213, doi:10.1029/2004GL019733.

——, M. N. Rajeevan, L. Zubair, and P. Yadav, 2011: Interannual variation of the South Asian monsoon: Links with ENSO and EQUINOO. *The Global Monsoon System: Research and Forecast*, 2nd ed. C.-P. Chang et al., Eds., World Scientific Series on Asia-Pacific Weather and Climate, Vol. 5, World Scientific, 25–42.

Ihara, C., Y. Kushnir, M. A. Cane, and V. H. De la Pena, 2007: Indian summer monsoon rainfall and its link with ENSO and the Indian Ocean climate indices. *Int. J. Climatol.*, **27**, 179–187, doi:10.1002/joc.1394.

Krishnamurthy, V., and J. Shukla, 2000: Intraseasonal and interannual variability of rainfall over India. *J. Climate*, **13**, 4366–4377, doi:10.1175/1520-0442(2000)013<0001:IAIVOR>2.0.CO;2.

Kumar, K. K., B. Rajagopalan, and M. A. Cane, 1999: On the weakening relationship between the Indian monsoon and ENSO. *Science*, **284**, 2156–2159, doi:10.1126/science.284.5423.2156.

Oza, M., and C. M. Kishtawal, 2014: Spatial analysis of Indian summer monsoon rainfall. *J. Geomatics*, **8** (1), 41–47.

Pant, G. B., and B. Parthasarathy, 1981: Some aspects of an association between the southern oscillation and Indian summer monsoon. *Arch. Meteor. Geophys. Bioclimatol.*, **29B**, 245–251, doi:10.1007/BF02263246.

Parthasarathy, B., A. A. Munot, and D. R. Kothawale, 1992: Indian summer monsoon rainfall indices: 1871–1990. *Meteor. Mag.*, **121**, 174–186.

——, ——, and ——, 1995: Monthly and seasonal rainfall series for all-India homogeneous regions and meteorological subdivisions: 1871–1994. Res. Rep. RR-065, Indian Institute of Tropical Meteorology, 113 pp.

Pattanaik, D. R., 2007a: Analysis of rainfall over different homogeneous regions of India in relation to variability in western movement frequency of monsoon depression. *Nat. Hazards*, **40**, 635–646, doi:10.1007/s11069-006-9014-0.

——, 2007b: Variability of convective activity over the northern Indian Ocean and its association with monsoon rainfall over India. *Pure Appl. Geophys.*, **164**, 1527–1545, doi:10.1007/s00024-007-0243-2.

Rasmusson, E. M., and T. H. Carpenter, 1983: The relationship between the eastern Pacific sea surface temperature and rainfall over India and Sri Lanka. *Mon. Wea. Rev.*, **111**, 517–528, doi:10.1175/1520-0493(1983)111<0517:TRBEEP>2.0.CO;2.

Sikka, D. R., and S. Gadgil, 1980: On the maximum cloud zone and the ITCZ over India longitude during the southwest monsoon. *Mon. Wea. Rev.*, **108**, 1840–1853, doi:10.1175/1520-0493(1980)108<1840:OTMCZA>2.0.CO;2.

Zhou, J., and K.-M. Lau, 2001: Principal modes of interannual and decadal variability of summer rainfall over South America. *Int. J. Climatol.*, **21**, 1623–1644, doi:10.1002/joc.700.